This document is a preprint of: P. Schulz, L. Scheuvens and G. Fettweis, "A New Perspective on Maximal-Ratio Combining," in Proceedings of IEEE International Symposium On Personal, Indoor And Mobile Radio Communications (PIMRC 2023), Toronto, Canada, Sep 2023. DOI:10.1109/PIMRC56721.2023.10293750

A New Perspective on Maximal-Ratio Combining

Philipp Schulz, Lucas Scheuvens, and Gerhard Fettweis
Vodafone Chair Mobile Communications Systems, Technische Universität Dresden, Dresden, Germany.
Email: {philipp.schulz2, lucas.scheuvens, fettweis}@tu-dresden.de,

***Abstract*—The realization of ultra-reliable low latency communications (URLLC) is a highly relevant problem that remains unsolved. Multi-connectivity (MC) is regarded as one of the main enablers as it has the potential to boost reliability by orders of magnitude. Typically, selection combining (SC) is implemented due to its simplicity. However, it is not optimal regarding the effective signal-to-noise ratio (SNR), in contrast to maximal-ratio combining (MRC). Furthermore, research focus is typically led on the outage probability only, but for reliable communications also the temporal behavior is relevant, which is better reflected by metrics like level crossing rate (LCR) and average fade duration (AFD). In this paper, we introduce a transformation which facilitates such an analysis by decoupling the dependence of the envelope or SNR from their time derivatives in MRC. Thereby, we present a thorough comparison between the investigated schemes of not only the outage but also the temporal behavior.**

***Index Terms*—Average fade duration (AFD), level crossing rate (LCR), maximal-ratio combining (MRC), multi-connectivity (MC), reliability**

I. Introduction

Since the discussion around the fifth generation of mobile networks (5G) began, ultra-reliable low latency communications (URLLC) has been a topic of significant interest among researchers [1], [2]. While public 5G is now widely available, it has primarily focused on delivering high data rates (similar to its predecessor 4G) and has not fully delivered on the promises of URLLC. Even private 5G measurement campaigns have failed to meet these requirements [3]: the achieved performance of 33 ms with 99.999 % or 15 ms with only 90 % probability are far away from the desired ultra-reliable 1 ms target. Requirements are set to increase even further with the upcoming sixth generation (6G) [4], making the achievement of URLLC a crucial challenge that remains unsolved.

Generally speaking, introducing redundancy is a well-known way to increase reliability, also in wireless communications. By transmitting redundant information distributed in space, time, and/or frequency, the added diversity can result in significant improvements in reliability.[1] One standardized approach to implement redundancy in URLLC is packet duplication [5], which involves transmitting copies of the same data over multiple paths simultaneously. The strongest link is then selected to retrieve the desired data using selection combining (SC). However, this technique can lead to energy wastage on the unused links. To address this issue, more sophisticated schemes have been proposed, such as coding methods, as demonstrated in [6], or coherent signal combining where the same data is transmitted, but the received signals are combined coherently. The optimal linear combiner that maximizes the resulting signal-to-noise ratio (SNR) is maximal-ratio combining (MRC) and was first introduced in [7].

Reliability requirements in URLLC are typically expressed in terms of outage probability, availability, or packet error rate (PER) values. These values are extremely low (or high for availability), often specified as five or more nines [4], and are challenging to validate through simulations or measurements. Consequently, mathematical models are a useful tool. For example, [8] presents an analytical framework to analyze multi-connectivity schemes, although it primarily focuses on the outage probability. However, newer works such as [9], [10] introduce novel dependability metrics that argue for the relevance of not only the pure outage probability but also the temporal behavior. This is because isolated errors typically have a different impact than burst errors. In this context, the level crossing rate (LCR) and the related average fade duration (AFD) can provide insights for a given outage threshold and form the basis for some of the aforementioned dependability metrics, which also take temporal behavior into account.

The concept of the LCR dates back to Rice's work in 1948 [11]. Consequently, the derived AFD can be considered as fundamental knowledge for single channels, as it can be found in standard textbooks [12]–[14]. However, results for MRC are scarce, mainly due to the fact that the signal envelope and its time derivative are not independent anymore, as is the case with single-link channels [15]. Thus, evaluating the LCR and AFD for MRC becomes more challenging. In spite of this, Beaulieu et al. provide results for the MRC's signal envelope in a Ricean channel, which also includes the Rayleigh channel as a special case [15]. However, defining a meaningful threshold for the LCR and AFD in the case of MRC is difficult, since MRC amplifies the signal and, consequently, the noise with different factors over time. Alternatively, expressions for the SNR would not only be more insightful but also allow for comparison with the non-amplified single connectivity or SC.

In this paper, we present two major contributions:

1) The introduction of a simple transformation on the envelope of the MRC signal to decouple it from its time derivative, facilitating the derivation of metrics like the LCR and AFD.
2) The inclusion of the SNR in the analysis to provide a meaningful perspective and make it comparable to other schemes, particularly single link and SC. Additionally, the authors provide an overview of the relevant metrics for all of these schemes.

[1]However, in the context of URLLC, the time domain might not be a suitable option due to the stringent latency demands.

© 2023 IEEE. Personal use of this material is permitted. Permission from IEEE must be obtained for all other uses, in any current or future media, including reprinting/republishing this material for advertising or promotional purposes, creating new collective works, for resale or redistribution to servers or lists, or reuse of any copyrighted component of this work in other works.

This document is a preprint of: P. Schulz, L. Scheuvens and G. Fettweis, "A New Perspective on Maximal-Ratio Combining," in Proceedings of IEEE International Symposium On Personal, Indoor And Mobile Radio Communications (PIMRC 2023), Toronto, Canada, Sep 2023. DOI:10.1109/PIMRC56721.2023.10293750

II. System Model

In this section we will set up the stage for our analysis, which will consider the perspective of a single user.

A. Single Link

For each link i, we consider the well-studied Rayleigh channel as the fading model. So the utilized properties are all textbook knowledge, which we will summarize here for convenience and in order to introduce our notation.

In this work, we are not interested in the complex signal s_i itself but rather in its derived metrics envelope r_i, power P_i, and the resulting SNR γ_i. First of all, we will consider the envelope r_i. Based on the assumptions of a Rayleigh channel, it can be derived that the envelope is Rayleigh distributed (hence, its name) [13, (3.32)], i. e.,

$$r_i := |s_i| \sim \text{Rayleigh}\left(\frac{\bar{P}_i}{2}\right) \tag{1}$$

and therefore, the probability density function (PDF) and cumulative distribution function (CDF) are given by

$$f_{r_i}(x) = \frac{2x}{\bar{P}_i} e^{-\frac{x^2}{\bar{P}_i}}, \qquad F_{r_i}(x) = 1 - e^{-\frac{x^2}{\bar{P}_i}}, \tag{2}$$

respectively. Therein, the only parameter is the average receive power $\bar{P}_i$. From this, the power distribution simply follows from the exchange of variables $P_i = r_i^2$ according to [13, (3.33)]

$$P_i = r_i^2 \sim \text{Exp}\left(\bar{P}_i^{-1}\right). \tag{3}$$

We may use $\lambda_i = \bar{P}_i^{-1}$ equivalently as a parameter for the exponential distribution.

Consequently, also the SNR is exponentially distributed, as it is the power scaled by the noise mean power N_0

$$\gamma_i = \frac{r_i^2}{N_0} \sim \text{Exp}\left(\bar{\gamma}_i^{-1}\right), \qquad \bar{\gamma}_i = \frac{\bar{P}_i}{N_0}. \tag{4}$$

From the SNR distribution, we can directly formulate an outage probability for a given SNR threshold $\hat{\gamma}$

$$O_{\hat{\gamma}} = \mathbb{P}\left[\gamma_i \leqslant \hat{\gamma}\right] = F_{\gamma_i}(\hat{\gamma}). \tag{5}$$

This definition also holds equivalently for the combining schemes discussed in Secs. III and IV.

In order to investigate the temporal behavior, we will also need the distribution of the envelope's time derivative, which is given in [14, (1.3-34)] as

$$\dot{r}_i := \frac{\mathrm{d}}{\mathrm{d}t} r_i \sim \mathcal{N}\left(0, \sigma_{\dot{r}_i}^2\right), \qquad \sigma_{\dot{r}_i}^2 = \pi^2 f_\mathrm{m}^2 \bar{P}_i. \tag{6}$$

Apart from the average receive power $\bar{P}_i$, this variance also depends on the maximum Doppler shift f_m. Accordingly, the PDF of $\dot{r}_i$ is expressed by

$$f_{\dot{r}_i}(x) = \frac{1}{\sqrt{2\pi^3 \bar{P}_i f_\mathrm{m}}} e^{-\frac{1}{2}\frac{x^2}{\pi^2 f_\mathrm{m}^2 \bar{P}_i}}. \tag{7}$$

In particular, [14] also states that the envelope r_i and its derivative $\dot{r}_i$ are independent.

B. LCR and AFD

We are now interested in metrics that characterize the temporal behavior of the system. In contrast to the distribution of the envelope r_i (or SNR γ_i or signal power P_i, respectively), which can only tell us, up to which probability (or to which time share) a metric will be below a certain threshold, the LCR and AFD provide the information on how often this happens and how long it takes on average.

In [11], Rice provides a formula of how many times a general signal x crosses a given threshold $\hat{x}$ from below per time unit, i. e., the LCR $L_{\hat{x}}$ for this threshold $\hat{x}$:

$$L_{\hat{x}} = \int_0^\infty y f_{x,\dot{x}}(\hat{x}, y) \mathrm{d}y. \tag{8}$$

It should be noted that even though this definition considers only the direction from below, the rate is obviously the same for the other direction, as the signal is continuous and every crossing from below comes with one from above. Further, it is worth noting that Eq. (8) requires the joint probability of the considered metric and its time derivative.

The AFD can then directly be calculated from the LCR [13, (3.46)] and the CDF as follows

$$T_{\hat{x}} = \frac{\mathbb{P}\left[x < \hat{x}\right]}{L_{\hat{x}}} = \frac{F_x(\hat{x})}{L_{\hat{x}}}. \tag{9}$$

Equipped with these fundamentals, we can now apply them on the envelope for a single link. Thanks to the independence stated at the end of Sec. II-A, Eq. (8) simplifies to

$$L_{\hat{r}} = f_r(\hat{r}) \int_0^\infty y f_{\dot{r}}(y) \mathrm{d}y = f_r(\hat{r}) \cdot \mathbb{E}\left[\dot{r} \mid \dot{r} > 0\right] \tag{10a}$$

$$= \frac{\hat{r} f_\mathrm{m} \sqrt{2\pi}}{\sqrt{\bar{P}}} e^{-\frac{\hat{r}^2}{\bar{P}}} = \rho_{\hat{r}} f_\mathrm{m} \sqrt{2\pi} e^{-\rho_{\hat{r}}^2} \tag{10b}$$

by inserting Eq. (2) and the expectation of the normally distributed derivative, conditioned on being positive. Therein, we used a similar short-hand notation $\rho_{\hat{r}} := \frac{\hat{r}}{\sqrt{\bar{P}}}$ as [13]. Inserting the LCR into Eq. (9) together with the exponential CDF from Eq. (2) the AFD is obtained as

$$T_{\hat{r}} = \frac{\sqrt{\bar{P}}}{\sqrt{2\pi} f_\mathrm{m} \hat{r}} \left(e^{\frac{\hat{r}^2}{\bar{P}}} - 1\right). \tag{11}$$

If we are now interested in these metrics for the SNR instead of the envelope, we can derive them by a simple transformation of the variable. Hence, for a given SNR threshold

$$\hat{\gamma} = \frac{\hat{r}^2}{N_0}, \tag{12}$$

we have $\hat{r} = \sqrt{\hat{\gamma} N_0}$ and therefore

$$L_{\hat{\gamma}} = \sqrt{2\pi \frac{\hat{\gamma}}{\bar{\gamma}}} f_\mathrm{m} e^{-\frac{\hat{\gamma}}{\bar{\gamma}}} = \sqrt{2\pi\zeta} f_\mathrm{m} e^{-\zeta}, \tag{13}$$

$$T_{\hat{\gamma}} = \frac{e^{\frac{\hat{\gamma}}{\bar{\gamma}}} - 1}{\sqrt{2\pi \frac{\hat{\gamma}}{\bar{\gamma}}} f_\mathrm{m}} = \frac{e^{\zeta} - 1}{\sqrt{2\pi\zeta} f_\mathrm{m}}. \tag{14}$$

Therein, we have introduced the ratio $\zeta = \frac{\hat{\gamma}}{\bar{\gamma}}$ of the SNR threshold to its mean.

© 2023 IEEE. Personal use of this material is permitted. Permission from IEEE must be obtained for all other uses, in any current or future media, including reprinting/republishing this material for advertising or promotional purposes, creating new collective works, for resale or redistribution to servers or lists, or reuse of any copyrighted component of this work in other works.

This document is a preprint of: P. Schulz, L. Scheuvens and G. Fettweis, "A New Perspective on Maximal-Ratio Combining," in Proceedings of IEEE International Symposium On Personal, Indoor And Mobile Radio Communications (PIMRC 2023), Toronto, Canada, Sep 2023. DOI:10.1109/PIMRC56721.2023.10293750

While for the single link the SNR is just a simple mapping where one envelope value corresponds to one SNR value, we will see in Sec. IV that in the MRC case, the situation will be different.

C. Multiple Links

In the analysis that follows in Secs. III and IV, we will extend the system model to L independent links, on which data can be transmitted in parallel in order to exploit diversity. The assumption of independence is crucial as it provides mathematical tractability, but also allows for the largest diversity gains. Even though this assumption is idealistic, it can be achieved to a great extent by using resources that are sufficiently separated in space (spatially distributed antennas) or frequency (using carriers separated by more than the coherence bandwidth). Further we restrict our analysis to links with the same average SNR $\bar{\gamma} = \bar{\gamma}_i$ (or same mean receive power $\bar{P} = \bar{P}_i$ and same noise power N_0, respectively), leading to independent and identically distributed (i.i.d.) random variables.

How exactly the data will be combined will be explained in the subsequent sections. However, both studied schemes can be described as a linear combiner

$$s = \sum_i \alpha_i s_i. \tag{15}$$

The studied multi-connectivity (MC) approaches all rely on the estimation of the individual links' SNRs γ_i. In this work, we assume that this estimation can be conducted perfectly.

III. Analysis of selection combining (SC)

As another baseline, we will also describe shortly the most simple diversity approach, wich is given by SC.

A. Preliminaries for SC

In SC, the receiver estimates the SNR of all links, and simply chooses the link $\hat{i}$ with the highest SNR

$$\hat{i} = \arg\max_i \gamma_i. \tag{16}$$

For the linear combiner in Eq. (15) this means that $\alpha_{\hat{i}} = 1$ and $\alpha_i = 0$ for all $i \neq \hat{i}$. Hence, the SNR is simply given as

$$\gamma_{\mathrm{SC}} = \gamma_{\hat{i}} = \max_i \gamma_i. \tag{17}$$

Due to the max operation, the following general relationships for the CDFs and PDFs of the maximum of several independent random variables X_i will become handy

$$F_{\max X_i}(x) = \mathbb{P}\left[\max X_i \leqslant x\right] = \prod_i F_{X_i}(x), \tag{18}$$

$$f_{\max X_i}(x) = \frac{\mathrm{d}}{\mathrm{d}t} F_{\max X_i}(x) = \sum_i f_{X_i}(x) \prod_{j \neq i} F_{X_j}(x). \tag{19}$$

If the L random variables are also identically distributed Eqs. (18) and (19) simplify as follows

$$F_{\max X_i}(x) = F_X(x)^L, \tag{20}$$

$$f_{\max X_i}(x) = L f_X(x) F_X(x)^{L-1}. \tag{21}$$

B. Two i.i.d. Links

Using Eqs. (20) and (21), we can directly express the CDF and PDF for the SC of two links with equal mean SNR as

$$F_{r_{\mathrm{SC}}}(x) = \left(1 - e^{-\frac{x^2}{\bar{P}}}\right)^2, \tag{22}$$

$$f_{r_{\mathrm{SC}}}(x) = \frac{4x}{\bar{P}} e^{-\frac{x^2}{\bar{P}}} \cdot \left(1 - e^{-\frac{x^2}{\bar{P}}}\right). \tag{23}$$

We observe that SC always chooses one of the signals and is identical to that signal until another signal becomes stronger. Therefore, except for these singular intersection points the derivative $\dot{r}_{\mathrm{SC}}$ of the combined signal, comes from one of the individual signals. This is true *almost everywhere*[2], such that the distribution of $\dot{r}_{\mathrm{SC}}$ is a mixture of the distributions of the individual $\dot{r}_i$. Due to the assumption of i.i.d. links and the independence of r_i and $\dot{r}_i$, we can even conclude that r_{SC} is independent from $\dot{r}_{\mathrm{SC}}$ and distributed exactly as the individual derivatives $\dot{r}_i$, and therefore $f_{\dot{r}_{\mathrm{SC}}} = f_{\dot{r}_i}$ as given in Eq. (7).

With this knowledge, we can easily derive the LCR of the envelope for a given threshold $\hat{r}$ as the joint PDF $f_{r,\dot{r}}$ is decoupled into the product of the individual PDFs

$$L_{\hat{r}} = f_r(\hat{r}) \int_0^\infty y f_{\dot{r}}(y) \mathrm{d}y \tag{24}$$

$$= 2\rho_{\hat{r}} e^{-\rho_{\hat{r}}^2} \cdot \left(1 - e^{-\rho_{\hat{r}}^2}\right) \cdot f_{\mathrm{m}} \sqrt{2\pi}. \tag{25}$$

Conseqently the AFD is given as

$$T_{\hat{r}} = \frac{F_r(\hat{r})}{L_{\hat{r}}} = \frac{e^{\rho_{\hat{r}}^2} - 1}{2\rho_{\hat{r}} \cdot f_{\mathrm{m}} \sqrt{2\pi}}. \tag{26}$$

Again, we can also provide the LCR and AFD for the SNR passing a given threshold $\hat{\gamma}$ by using the same transformation as for Eqs. (13) and (14)

$$L_{\hat{\gamma}} = 2\left(1 - e^{-\zeta}\right) \cdot \sqrt{2\pi\zeta} f_{\mathrm{m}} e^{-\zeta}, \tag{27}$$

$$T_{\hat{r}} = \frac{e^{\zeta} - 1}{2 f_{\mathrm{m}} \sqrt{2\pi\zeta}}. \tag{28}$$

IV. Analysis of maximal-ratio combining (MRC)

Similarly to the previous sections we will now study the same metrics for the MRC scheme.

A. Preliminaries for MRC

For the implementation of MRC the signals are co-phased such that the weighting factors α_i look like

$$\alpha_i = a_i e^{-i\theta_i}. \tag{29}$$

Thanks to the co-phasing, we do not look into the complex signal anymore, but only study the real valued envelope

$$r_{\mathrm{MRC}} = \sum a_i r_i. \tag{30}$$

[2]Sounding a bit unscientific, this is really meant in the mathematical sense, meaning that the singular points have a probability of zero.

© 2023 IEEE. Personal use of this material is permitted. Permission from IEEE must be obtained for all other uses, in any current or future media, including reprinting/republishing this material for advertising or promotional purposes, creating new collective works, for resale or redistribution to servers or lists, or reuse of any copyrighted component of this work in other works.

This document is a preprint of: P. Schulz, L. Scheuvens and G. Fettweis, "A New Perspective on Maximal-Ratio Combining," in Proceedings of IEEE International Symposium On Personal, Indoor And Mobile Radio Communications (PIMRC 2023), Toronto, Canada, Sep 2023. DOI:10.1109/PIMRC56721.2023.10293750

The aim of MRC is now to choose the weights a_i wisely, such that the resulting SNR is maximized. Following [13] we can derive the following SNR

$$\gamma_{\mathrm{MRC}} = \frac{r_{\mathrm{MRC}}^2}{N_{\mathrm{tot}}} = \frac{1}{N_0}\frac{\left(\sum a_i r_i\right)^2}{\sum a_i^2} \tag{31}$$

$$\leqslant \frac{1}{N_0}\sum r_i^2 = \sum \frac{r_i^2}{N_0} = \sum \gamma_i. \tag{32}$$

The inequality is a result of applying the Cauchy-Schwarz inequality to the numerator. The Cauchy-Schwarz inequality also tells us that equality is achieved if and only if the weights are set as $a_i^2 = \frac{r_i^2}{N_0}$ (or scaled versions of that). That is why MRC is achieved, when all links are multiplied by their SNRs.

Now, the weights can be inserted into Eq. (30) in order to obtain the envelope and its time derivative

$$r_{\mathrm{MRC}} = \sum a_i r_i = \frac{1}{\sqrt{N_0}}\sum r_i^2 = \sqrt{N_0}\gamma_{\mathrm{MRC}}, \tag{33}$$

$$\dot{r}_{\mathrm{MRC}} = \frac{2}{\sqrt{N_0}}\sum r_i \dot{r}_i. \tag{34}$$

What is often forgotten here is the fact that this combined signal is an amplified signal and so also the noise is amplified, as illustrated in Fig. 1. As can be seen in Fig. 1(a), a threshold $\hat{r}$ on the envelope would be suitable for a comparison of the individual links and SC, since they all experience the same noise power. However, for MRC also the noise level raises due to the weighting factors. In contrast, Fig. 1(b) shows the SNR, which incorporates also the (amplified) noise. Hence, the LCR and AFD are only meaningful for the SNR in order to achieve a fair comparison.

As we consider i.i.d. links, all SNRs are exponentially distributed with the same mean, and since γ_{MRC} is the sum of the single SNRs, as shown in Eq. (32), it follows a Gamma distribution

$$\gamma_{\mathrm{MRC}} \sim \Gamma(L, \bar{\gamma}), \tag{35}$$

$$f_{\gamma_{\mathrm{MRC}}}(x) = \frac{x^{L-1}}{(L-1)!\cdot\bar{\gamma}^L}e^{-\frac{x}{\bar{\gamma}}}. \tag{36}$$

From this, we can also derive the PDF of the envelope by transforming via the relationship given in Eq. (33)

$$f_{r_{\mathrm{MRC}}}(x) = f_{\gamma_{\mathrm{MRC}}}\left(\frac{x}{\sqrt{N_0}}\right)\frac{1}{\sqrt{N_0}} \tag{37}$$

$$= \frac{x^{L-1}}{(L-1)!\cdot\sqrt{N_0}^L\cdot\bar{\gamma}^L}e^{-\frac{x}{\sqrt{N_0}\bar{\gamma}}}. \tag{38}$$

For our analysis we will also need the distribution of the envelope's square root

$$\varrho := \sqrt{r_{\mathrm{MRC}}} = \sqrt[4]{N_0}\sqrt{\gamma_{\mathrm{MRC}}}, \tag{39}$$

whose PDF can be obtained by another transformation

$$f_\varrho(x) = f_{\sqrt{r_{\mathrm{MRC}}}}(x) = f_{r_{\mathrm{MRC}}}\left(x^2\right)\cdot 2x \tag{40}$$

$$= \frac{2x^{2L-1}}{(L-1)!\cdot\sqrt{N_0}^L\cdot\bar{\gamma}^L}e^{-\frac{x^2}{\sqrt{N_0}\bar{\gamma}}}. \tag{41}$$

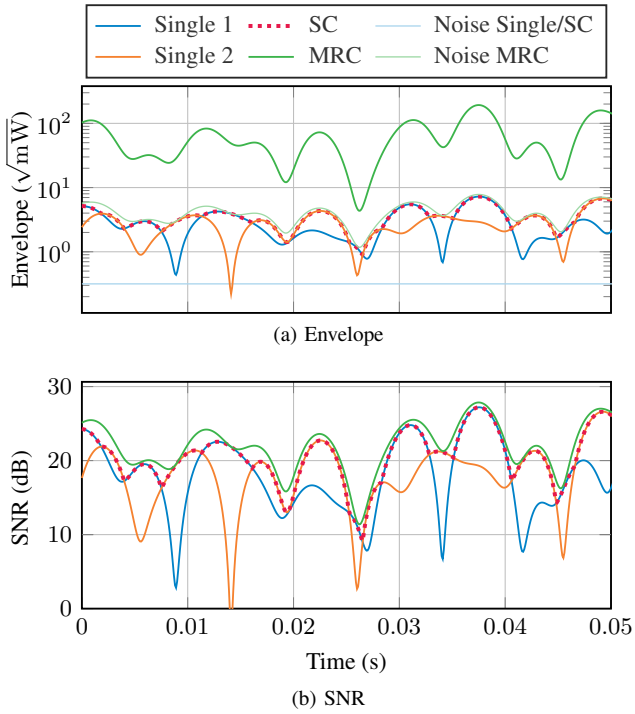

(a) Envelope

(b) SNR

Fig. 1: Channels and combined channels over time.

B. Two i.i.d. Links

We will now study the special case of two i.i.d. links. As it becomes evident in Eqs. (33) and (34), the independence of the envelope r_{MRC} and its time derivative $\dot{r}_{\mathrm{MRC}}$ cannot be stated anymore, since both depend on the individual envelopes r_i. Without the independence property, evaluating Rice's formula in Eq. (8) becomes cumbersome. To overcome this problem, we propose in this work to look at the auxiliary variable ϱ as introduced in Eq. (39), which will turn out later to lead to a decoupling.

For two links, the newly introduced auxiliary variables are expressed as follows.

$$\varrho = \sqrt{r_{\mathrm{MRC}}} = \frac{1}{\sqrt[4]{N_0}}\cdot\sqrt{r_1^2 + r_2^2} =: \frac{1}{\sqrt[4]{N_0}}\cdot\xi, \tag{42}$$

$$\dot{\varrho} := \frac{\mathrm{d}}{\mathrm{d}t}\sqrt{r_{\mathrm{MRC}}} = \frac{1}{\sqrt[4]{N_0}}\cdot\frac{r_1\dot{r}_1 + r_2\dot{r}_2}{\sqrt{r_1^2 + r_2^2}} =: \frac{1}{\sqrt[4]{N_0}}\cdot\eta. \tag{43}$$

In these equations, we have introduced two further auxiliary variables, ξ and η, in order to not carry the noise factor through all following derivations.

From Eq. (41) we can extract the PDF of ϱ for two links

$$f_\varrho(x) = \frac{2x^3}{N_0\cdot\bar{\gamma}^2}e^{-\frac{x^2}{\sqrt{N_0}\bar{\gamma}}}. \tag{44}$$

We will now see that we will be able to express $\dot{\varrho}$ independently from all r_i. Therefore, we look at the auxiliary variable η

$$\eta = \frac{r_1}{\sqrt{r_1^2 + r_2^2}}\dot{r}_1 + \frac{r_2}{\sqrt{r_1^2 + r_2^2}}\dot{r}_2 \tag{45}$$

$$= \beta\dot{r}_1 + \sqrt{1-\beta^2}\dot{r}_2. \tag{46}$$

© 2023 IEEE. Personal use of this material is permitted. Permission from IEEE must be obtained for all other uses, in any current or future media, including reprinting/republishing this material for advertising or promotional purposes, creating new collective works, for resale or redistribution to servers or lists, or reuse of any copyrighted component of this work in other works.

This document is a preprint of: P. Schulz, L. Scheuvens and G. Fettweis, "A New Perspective on Maximal-Ratio Combining," in Proceedings of IEEE International Symposium On Personal, Indoor And Mobile Radio Communications (PIMRC 2023), Toronto, Canada, Sep 2023. DOI:10.1109/PIMRC56721.2023.10293750

By introducing the coefficient $\beta = \frac{r_1}{\xi}$ we have already reduced r_1 and r_2 to one parameter.[3] It remains to show that the random variable β is independent from r_i, because then η (and therefore $\dot{\varrho}$) is independent from ϱ.

As a first step, we look at the distribution of ξ. Therefore, we start with ξ^2

$$\xi^2 = r_1^2 + r_2^2 \quad \sim \Gamma(2, \bar{P}) \tag{47}$$
$$f_{\xi^2}(x) = \lambda^2 x e^{-\lambda x}, \tag{48}$$

and obtain the PDF of ξ through the transformation

$$f_{\xi}(x) = f_{\xi^2}(x^2) \cdot 2x = 2x^3 \lambda^2 e^{-\lambda x^2}. \tag{49}$$

We then study the distribution of ξ for a fixed value of r_1. From the conditioned CDF

$$F_{\xi|r_1}(x) = \mathbb{P}\left[\xi \leqslant x \mid r_1\right] = \mathbb{P}\left[r_2^2 \leqslant x^2 - r_1^2 \mid r_1\right] \tag{50}$$
$$= F_{r_2^2}\left(x^2 - r_1^2\right), \tag{51}$$

the conditioned PDF can be obtained as

$$f_{\xi|r_1=x}(y) = \begin{cases} 0, & x < r_1, \\ 2x\lambda e^{-\lambda\left(x^2 - r_1^2\right)}, & x \geqslant r_1. \end{cases} \tag{52}$$

Using Bayes' formula, this can be translated into the distribution of r_1 conditioned on ξ

$$f_{r_1|\xi=y}(x) = \frac{f_{\xi|r_1=x}(y) f_{r_1}(x)}{f_{\xi}(y)} \tag{53}$$
$$= \frac{2y\lambda e^{-\lambda\left(y^2 - x^2\right)} \cdot 2x\lambda e^{-\lambda x^2}}{2y^3\lambda^2 e^{-\lambda y^2}} = \frac{2}{y^2} x \tag{54}$$
$$F_{r_1|\xi=y}(x) = \frac{x^2}{y^2} \tag{55}$$

for $0 < x \leqslant y$. For other values of x the expression is simply zero. Finally, this brings us to the conditioned CDF of β

$$F_{\beta|\xi=y}(x) = \mathbb{P}\left[\beta = \frac{r_1}{\xi} \leqslant x \,\middle|\, \xi = y\right] \tag{56}$$
$$= \mathbb{P}\left[r_1 \leqslant x\xi \mid \xi = y\right] = F_{r_1|\xi=y}(x\xi) = x^2. \tag{57}$$

As can be seen, the distribution of β conditioned on ξ is completely decoupled from ξ, such that both variables are independent and $F_\beta = F_{\beta|\xi}$. Accordingly, the PDF is simply given as

$$f_\beta(x) = 2x, \qquad 0 \leqslant x \leqslant 1. \tag{58}$$

In particular, it becomes evident that β is not only independent from ξ, but also from r_i and $\dot{r}_i$.

Now that we know the independence, we can study Eq. (46), which is a sum of independent normal variables. Thus, for a fixed β, we have

$$\eta_{|\beta} \sim \mathcal{N}\left(0, \left(\beta^2\sigma_1^2 + (1-\beta^2)\sigma_2^2\right)\right) = \mathcal{N}\left(0, \sigma_{\dot{r}}^2\right), \tag{59}$$

[3]The geometrical interpretation of this approach is a right triangle with the legs r_1 and r_2. Then the coefficients of $\dot{r}_1$ and $\dot{r}_2$ in Eq. (45) refer to the sine and cosine in such a triangle.

TABLE I: Simulation Parameters

Average SNR	$\bar{\gamma}$	20 dB	
Number of samples	N_s	10^7	
Sampling time	T_s	0.1 ms	
Max. Doppler frequency	f_m	100 Hz	
Coherence time	T_coh	4.2 ms	[16, (4.40c)]

since $\sigma_1^2 = \sigma_2^2 = \sigma_{\dot{r}}^2$. Hence, η is independent from β

$$\eta \sim \mathcal{N}\left(0, \sigma_{\dot{r}}^2\right). \tag{60}$$

Finally, we obtain the distribution and variance of $\dot{\varrho}$ as

$$\dot{\varrho} = \frac{1}{\sqrt[4]{N_0}}\eta \sim \mathcal{N}\left(0, \frac{1}{\sqrt{N_0}}\sigma_{\dot{r}}^2\right), \quad \sigma_{\dot{\varrho}}^2 = \frac{1}{\sqrt{N_0}}\pi^2 f_\mathrm{m}^2 \bar{P}. \tag{61}$$

C. LCR and AFD for MRC of Two i.i.d. Links

Thanks to our decoupling of variable and derivative by introducing ϱ, we are in the comfortable situation that the Rice formula for the LCR of the envelope's square root crossing a threshold $\hat{\varrho}$ again falls into two factors

$$L_{\hat{\varrho}} = f_\varrho(\hat{\varrho}) \int_0^\infty y f_{\dot{\varrho}}(y)\mathrm{d}y = f_\varrho(\hat{\varrho})\sigma_{\dot{\varrho}}\sqrt{\frac{2}{\pi}}. \tag{62}$$

However, we are interested in the SNR and so we transform the threshold by $\hat{\varrho}(\hat{\gamma}) = \sqrt[4]{N_0}\sqrt{\hat{\gamma}}$ and obtain

$$L_{\hat{\gamma}} = f_\varrho\left(\sqrt[4]{N_0}\sqrt{\hat{\gamma}}\right)\frac{\sigma_{\dot{\varrho}}}{2}\sqrt{\frac{2}{\pi}} \tag{63}$$
$$= \frac{\left(\sqrt{\hat{\gamma}}\right)^3}{\sqrt[4]{N_0}\cdot\bar{\gamma}^2} e^{-\frac{\hat{\gamma}}{\bar{\gamma}}} \frac{1}{\sqrt[4]{N_0}}\pi f_\mathrm{m}\sqrt{\bar{P}_i}\sqrt{\frac{2}{\pi}} \tag{64}$$
$$= \zeta^{\frac{3}{2}} e^{-\zeta} f_\mathrm{m}\sqrt{2\pi}. \tag{65}$$

Consequently, the AFD directly follows as

$$T_{\hat{\varrho}} = \frac{\mathbb{P}\left[\gamma_\mathrm{MRC} < \hat{\gamma}\right]}{L_{\hat{\gamma}}} = \frac{F_{\gamma_\mathrm{MRC}}(\hat{\gamma})}{L_{\hat{\gamma}}} = \frac{\boldsymbol{\gamma}\left(2,\zeta\right)e^{\zeta}}{\zeta^{\frac{3}{2}} f_\mathrm{m}\sqrt{2\pi}}, \tag{66}$$

where $\boldsymbol{\gamma}$ denotes the lower incomplete gamma function.

V. Numerical Validation and Evaluation

The analytical results will now be validated by comparing them with numerical simulations.

A. Simulation Scenario

In order to validate the derived models, we used Matlab 2022b and its implementation of a Rayleigh channel from the communications toolbox. It was configured to utilize the sum of sinusoids technique and Jakes' Doppler spectrum. Further simulation parameters are summarized in Table I.

B. Distributions of MRC Metrics

Firstly, we study the distributions of the envelope, its square root, and the respective time derivatives for the MRC scheme in Fig. 2. Here, the SNR is not considered separately, since in this case it is simply a scaled version of the envelope (cf. Eq. (33)). The figure confirms a good agreement of the empirical histograms and the model PDFs, where available. We could not provide a model for the envelope's derivative $\dot{r}_\mathrm{MRC}$ in Fig. 2(b), but our proposed auxiliary variable ϱ provided a simple and accurate model for the derivative $\dot{\varrho}$ in Fig. 2(d).

© 2023 IEEE. Personal use of this material is permitted. Permission from IEEE must be obtained for all other uses, in any current or future media, including reprinting/republishing this material for advertising or promotional purposes, creating new collective works, for resale or redistribution to servers or lists, or reuse of any copyrighted component of this work in other works.

This document is a preprint of: P. Schulz, L. Scheuvens and G. Fettweis, "A New Perspective on Maximal-Ratio Combining," in Proceedings of IEEE International Symposium On Personal, Indoor And Mobile Radio Communications (PIMRC 2023), Toronto, Canada, Sep 2023. DOI:10.1109/PIMRC56721.2023.10293750

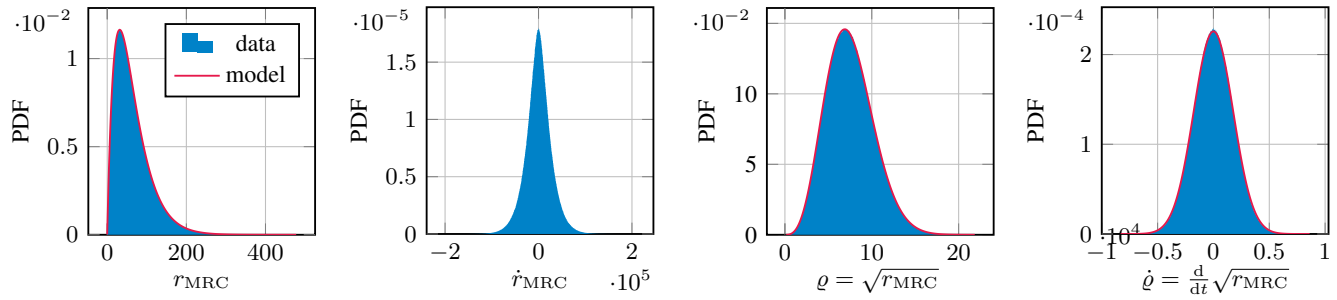

(a) (b) (c) (d)

Fig. 2: Comparison of the empirical distributions from simulations with the derived models (where available) for the envelope r_{MRC} and the square-rooted envelope ϱ as well as their derivatives in MRC. The legend applies to all plots.

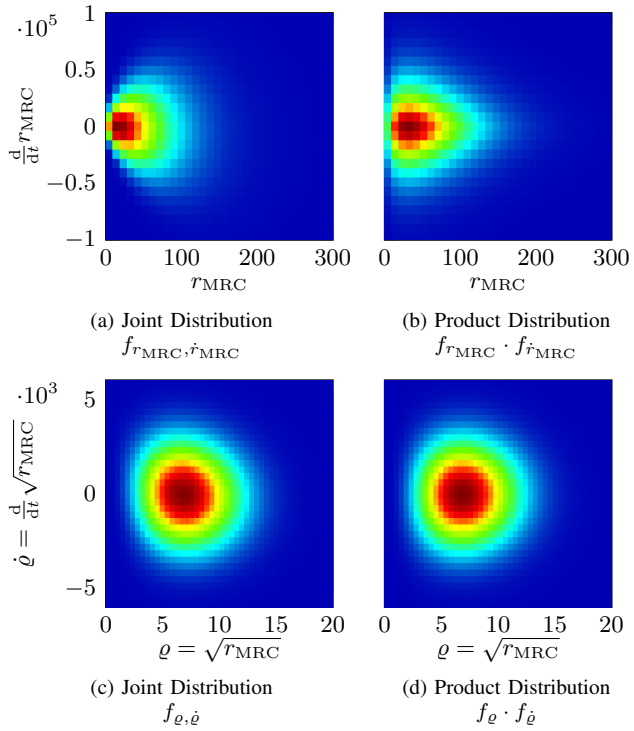

(a) Joint Distribution $f_{r_{\mathrm{MRC}},\dot{r}_{\mathrm{MRC}}}$

(b) Product Distribution $f_{r_{\mathrm{MRC}}} \cdot f_{\dot{r}_{\mathrm{MRC}}}$

(c) Joint Distribution $f_{\varrho,\dot{\varrho}}$

(d) Product Distribution $f_{\varrho} \cdot f_{\dot{\varrho}}$

Fig. 3: Joint vs. product distributions from simulations.

C. Joint Distributions and Independence

Next, we want to have a look at Fig. 3. Therein, we show the empirical joint and product distribution of the envelope r_{MRC} and the envelope's square root ϱ with their time derivatives, respectively. The empirical joint distributions in Figs. 3(a) and 3(c) are obtained as a two-dimensional histogram. In contrast, for the product distributions in Figs. 3(b) and 3(d) the histograms have been generated for both components separately and multiplied afterwards.

Per definition, two random variables $X \in \mathcal{X}$ and $Y \in \mathcal{Y}$ are independent, if they fulfill

$$f_{X,Y}(x,y) = f_X(x) \cdot f_Y(y) \qquad \forall x \in \mathcal{X}, y \in \mathcal{Y}. \tag{67}$$

However, by comparing Figs. 3(a) and 3(b) it can be visually observed that the shapes are systematically different: The left plot opens like a fan, whereas the right plot is more triangular shaped. In contrast, if we look at the plots of the proposed transformation in Figs. 3(c) and 3(d), the results are the same apart from some numerical and stochastic noise. In particular, there is no systematic error visible.

Of course, these plots are only an empirical observation and the differences may be more or less severe for different parameters, but the empirical data support the analytical statements deducted in Sec. IV.

D. Outage, LCR, and AFD

Finally, we study how well our derivations allow us to calculate the performance metrics outage, LCR, and AFD for MRC. The results are shown in Fig. 4, where markers and lines show results from simulations and models, respectively. The dashed line shows the single link result for the doubled SNR, which refers to an (approx.) 3 dB shift in the x direction. This comparison is more fair, because it reflects the same total power for the single link scheme as in the combined schemes. However, the other comparison is also meaningful, because the maximum power per link might be regulated.

We can make the following observations. First of all, the models match the simulation results almost perfectly, which was our primary goal. A small mismatch appears only for the smaller SNR thresholds, where the simulation accuracy suffers as outage and fade durations are harder to observe when the signal falls below the threshold only extremely rarely (As can be seen, there are no fades observed by the two combining schemes at all for $\hat{\gamma} < -12\,\mathrm{dB}$ and hence no data points for LCR and AFD). However, the models allow also to look into these regions relevant for URLLC.

In Fig. 4(a), the expected behavior can be observed. The MC schemes leverage the outage by orders of magnitude (e. g., from 10^{-2} to 10^{-4} at $\hat{\gamma} = 0\,\mathrm{dB}$). As the outage probability scales with O^L for SC (and even better for MRC), the MC schemes benefit even more for small tolerated SNR thresholds $\hat{\gamma}$, where the single link outage is already low. In particular, it becomes evident that increasing the transmit power in the single link scheme by factor two results in the same total power but hardly brings benefits as compared to the MC schemes. However, for large thresholds the gains diminish, so none of the schemes can compensate small fading margins.

© 2023 IEEE. Personal use of this material is permitted. Permission from IEEE must be obtained for all other uses, in any current or future media, including reprinting/republishing this material for advertising or promotional purposes, creating new collective works, for resale or redistribution to servers or lists, or reuse of any copyrighted component of this work in other works.

This document is a preprint of: P. Schulz, L. Scheuvens and G. Fettweis, "A New Perspective on Maximal-Ratio Combining," in Proceedings of IEEE International Symposium On Personal, Indoor And Mobile Radio Communications (PIMRC 2023), Toronto, Canada, Sep 2023. DOI:10.1109/PIMRC56721.2023.10293750

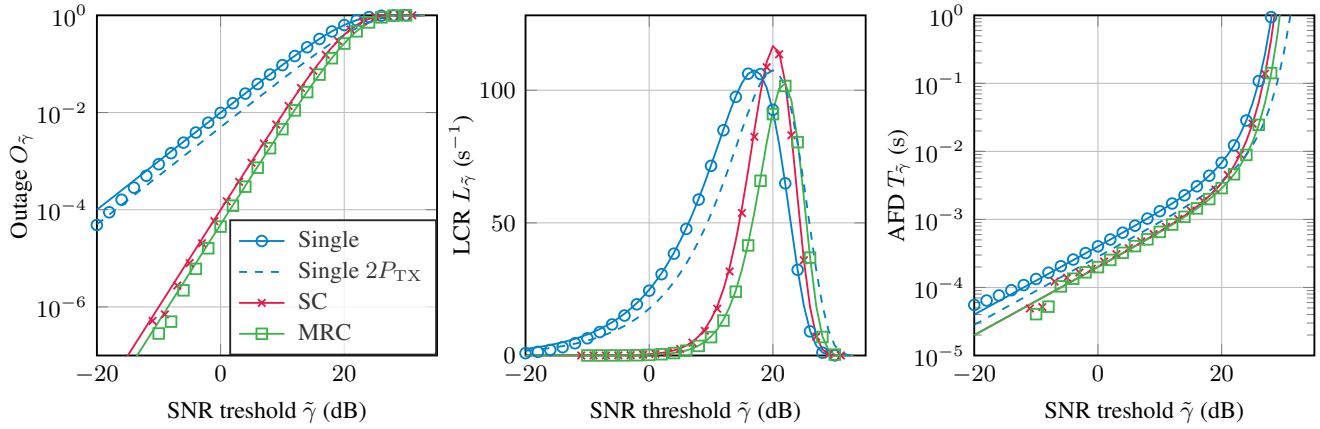

(a) Outage (b) LCR (c) AFD

Fig. 4: Performance of the investigated schemes and validation of the models (lines) with simulation data (markers). The legend applies to all plots.

As for the LCR in Fig. 4(b), we can observe that the MC schemes can maintain very low rates up to $\hat{\gamma} \approx 10\,\mathrm{dB}$. This is due to the fact that deep fades are much less likely for these schemes as can be seen in Fig. 1(b). In the short interval depicted there, $\hat{\gamma} \approx 10\,\mathrm{dB}$ is never touched by the MC schemes, but the single link curves cross it several times. Here, doubling the power of a single link also does not really help, as the deep fades remain deep after a 3 dB shift. Only for higher thresholds, the LCRs are comparable.

Finally, in Fig. 4(c) almost parallel curves for the AFD can be observed, especially in the region $\hat{\gamma} < 20\,\mathrm{dB}$, where the lines are almost linear (in the log scale) and parallel. The distance is roughly a factor of two in this region, which would translate to twice as many consecutive packet errors. For higher thresholds, the curves converge, only the dashed line keeps its distance, as it is only a shifted version of the single link line. Hence, a single link with twice the power would be even superior over the MC schemes with respect to the AFD for high SNR thresholds. However, this region is less interesting for URLLC.

VI. Conclusion and Outlook

By introducing the transformation by a square root we have decoupled the envelope (or the signal-to-noise ratio (SNR)) and its time derivative in maximal-ratio combining (MRC), facilitating further analysis, e. g., to derive the level crossing rate (LCR) and average fade duration (AFD). We stated the importance of studying and comparing the SNR, since in MRC not only the signal but also the noise is amplified and, thus, thresholds on the envelope are not comparable to other schemes. Accordingly, we conducted the analysis for single links, selection combining (SC), and MRC and were able to compare not only outage but also the temporal behavior for single links, SC, and MRC.

This work is mainly about the introduction of the square root transformation and was therefore exemplary conducted with two links and Rayleigh fading as a simple model. Future studies will generalize the models in these regards.

Acknowledgment

This work was funded and supported by the project "Industrial Radio Lab Germany (IRLG)" under contract 16KIS1010K, funded by the Federal Ministry of Education and Research, Germany.

References

[1] ITU-R, "IMT vision – framework and overall objectives of the future development of IMT for 2020 and beyond," International Telecommunication Union - Radiocommunication Sector, Rec. ITU-R M.2083-0, 9 2015.

[2] P. Popovski *et al.*, "Wireless access in ultra-reliable low-latency communication (URLLC)," *IEEE Trans. Commun.*, vol. 67, no. 8, pp. 5783–5801, 2019.

[3] J. Rischke, P. Sossalla, S. Itting, F. H. P. Fitzek, and M. Reisslein, "5G campus networks: A first measurement study," *IEEE Access*, vol. 9, pp. 121 786–121 803, 2021.

[4] M. Latva-aho and K. Leppänen, "Key drivers and research challenges for 6G ubiquitous wireless intelligence," 6G Flagship, White Paper, 9 2019.

[5] 3GPP, "3rd generation partnership project; technical specification group services and system aspects; release 15 description; summary of rel-15 work items (release 15)," Tech. Rep. TR 21.915 V15.5.0, 2019.

[6] P. Schulz, A. Traßl, A. N. Barreto, and G. Fettweis, "Efficient and reliable wireless communications via multi-connectivity using rateless codes in single-and multi-user scenarios," *IEEE Trans. Commun.*, vol. 20, no. 9, pp. 5714–5729, Apr 2021.

[7] L. R. Kahn, "Ratio squarer," *Proceedings of the IRE (Correspondence)*, vol. 42, no. 11, pp. 1698–1704, 1954.

[8] A. Wolf, P. Schulz, M. Dörpinghaus, J. C. S. Santos Filho, and G. Fettweis, "How reliable and capable is multi-connectivity?" *IEEE Trans. Commun.*, vol. 67, no. 2, pp. 1506–1520, 2019.

[9] T. Hößler, P. Schulz, M. Simsek, and G. P. Fettweis, "Mission availability for wireless URLLC," in *2019 IEEE Global Communications Conference (GLOBECOM)*, 2019, pp. 1–6.

[10] I. Muhammad, H. Alves, N. H. Mahmood, O. L. A. López, and M. Latva-aho, "Mission effective capacity—a novel dependability metric: A study case of multiconnectivity-enabled URLLC for IIoT," *IEEE Trans. Ind. Informat.*, vol. 18, no. 6, pp. 4180–4188, 2022.

[11] S. O. Rice, "Statistical properties of a sine wave plus random noise," *The Bell System Technical Journal*, vol. 27, no. 1, pp. 109–157, 1948.

[12] G. L. Stüber, *Principles of Mobile Communication*, 4th ed. Springer, 2017.

[13] A. Goldsmith, *Wireless Communications*, 1st ed. Cambridge University Press, 2005.

[14] W. C. Jakes, *Microwave Mobile Communications*. Wiley, 1994.

[15] N. Beaulieu and X. Dong, "Level crossing rate and average fade duration of MRC and EGC diversity in Ricean fading," *IEEE Trans. Commun.*, vol. 51, no. 5, pp. 722–726, 2003.

[16] T. S. Rappaport, *Wireless communications principles and practice*, 2nd ed. Upper Saddle River, NJ: Prentice Hall, 2002.

© 2023 IEEE. Personal use of this material is permitted. Permission from IEEE must be obtained for all other uses, in any current or future media, including reprinting/republishing this material for advertising or promotional purposes, creating new collective works, for resale or redistribution to servers or lists, or reuse of any copyrighted component of this work in other works.